Behavior of Self-assembled Mn(III)/Mn(II)-NEt$_3$ Conjugate on Different Support Observed by AFM-SNOM

Alexander Vasil'evich Udal'tsov

Faculty of Biology, Lomonosov Moscow State University, Moscow119899, Russian Federation

Abstract: Et$_3$N (Mn^{II}-triethylamine) complex conjugated with binuclear Mn^{III}-hydroxide, Mn$_2$(OH)$_3$Cl and similar manganese complex with Et$_2$NH (diethylamine) self-assembled in aqueous solutions have been investigated by simultaneous AFM (atomic force microscopy) and SNOM (scanning near-field optical microscopy) in thin layers prepared on mica and PET (polyethylene terephthalate). The size of the particles after crystallization of the precipitated former conjugate was controlled with XRD (X-ray diffraction). It is found that the conjugate self-assembling produces the smallest grains with the diameter of 65 ± 7.5 nm measured at contact with the support. This particle size matches the crystallite size of 44.2 nm found by XRD for the conjugate taking into account the particles deformation under the contact with the support. The self-assembly of the smallest particles in solution has produced non-transparent for light core observed on mica with the size varied between 300 to 400 nm. The latter occurs due to hydrophobic interactions since no core of the former conjugate has been found on hydrophobic PET surface. No submicroscopic core is also found in the case of similar conjugate with Mn^{II}-Et$_2$NH complex on PET film and mica both.

Key words: Mn^{II}-NEt$_3$ complex, conjugate with Mn^{III}-hydroxide, self-assembling, simultaneous AFM-SNOM.

1. Introduction

Various means of microscopy including such as simultaneous AFM (atomic force microscopy) and SNOM (scanning near-field optical microscopy) play important role in comprehensive characterization of nanomaterials providing their visualization [1-4]. The simultaneous optical scanning together with the topography probing provides useful appropriate image exhibiting further morphology details of a supramolecular structure. SNOM was previously called photon STM (scanning tunneling microscopy) since it reflects the main feature, when the light penetrates through aqueous covers of hydrated substance revealing substantial details on the surface. Thus, it complements submicroscopic techniques of AFM that records topography of a rough surface. Therefore, AFM-SNOM as a photophysical tool admits the local identification of different species in minute quantities prepared in thin layers and the surface

hydration [5, 6]. As a result, this photophysical tool is widely applied in biology, photochemistry, and material science.

The scanning probe microscopy is also useful for the study of self-assembled structures producing nanorods, nanosheets, nanocrystals, and so on [7-10]. It is interesting that the crystallization of self-organized assemblies of mono-protonated TPP (*meso*-tetraphenyl-porphine) dimers in thin layers, which contain the confined water, has own remarkable features as found earlier by AFM [11]. Among different Mn-based complexes, the complex formed by Mn^{II} and Et$_3$N has exhibited unordinary behavior since this complex is involved in the conjugate with binuclear Mn^{III} hydroxide [12]. Earlier our studies of manganese complexes with aliphatic amines, Et$_2$NH and Et$_3$N were carried out by electronic and infrared spectroscopy and scanning probe microscopy [13, 14]. However, the conjugation between Mn^{II}-NEt$_3$ complex and a Mn^{III}-hydroxide and for the other one with Et$_2$NH has not been found. The view of quite unstable complex formed by aliphatic amines and manganese

---

Corresponding author: Alexander Vasil'evich Udal'tsov, Ph.D., researcher, research field: materials science engineering.

aquacomplex [15] actually suggests Mn^{II} transformation to higher oxidative states in the presence of dioxygen in a solution. In fact the interaction between the reagents, $MnCl_2$ and Et_3N or Et_2NH in aqueous solution leads to the formation of $C-N(H_3O)^+$ groups and $Mn^{III}-OH$ species that implies the interaction between the ligands resulting in the hydrogen bonding [12]. Thus, further study of these molecular systems produced after the interaction between $MnCl_2$ and Et_3N (or Et_2NH) by simultaneous AFM-SNOM in combination with X-ray diffraction should clarify details of the compounds self-assembling, the results of which are reported in the present paper.

2. Experimental Section

Aldrich diethylamine (Et_2NH), triethylamine (Et_3N), and $MnCl_2 \cdot 4H_2O$, and distilled water were used for the preparation of $MnCl_2$ solutions and the complexes with amine. Thin layers of Mn^{III}-hydroxide/Mn^{II}-NEt₃ conjugate were prepared on mica or PET (polyethylene terephthalate) film by evaporation of the solvent from 4.0×10^{-3} mol·L⁻¹ $MnCl_2$ and 4.0×10^{-3} mol·L⁻¹ Et_3N solution. Similar concentrations were used in the case of Et_3NH as a ligand.

2.1 Isolation of Mn^{II}-NEt₃ Complex and Crystallization

The liquid over the white-gel precipitate obtained after its separation by centrifugation was slowly evaporated at room temperature during two weeks until its color became yellow-green. Then the crystallization of this viscous solution produced manganese containing yellow-green crystals, which were analyzed by IR spectroscopy and XRD. X-ray diffraction pattern of the yellow-green crystals has exhibited characteristic intense diffraction lines with d(Å) = 4.37; 3.29; 2.62, and 2.18 equally distanced via $2\Theta = 6.9° \pm 0.2°$ from each other. According to X-ray fluorescence analysis with an analyzer Mesa-500W (Horiba, Japan) and IR spectra its formula was found to be

$[Mn^{2+}(Et_3N)_3(H_3O)^+]Cl^-_3$ [12]. At the same time this complex contained water in the coordination shell, number of which has been found to be 8 per one Mn^{II} [12]. Thus, Mn^{II} in this water-soluble complex formed by Et_3N and $MnCl_2$ in the aqueous solution has not been oxidized by O_2.

2.2 Preparation of Molecular Conjugate of Mn^{II}-NEt₃ Complex and Mn₂Cl(OH)₃ for X-ray Diffraction

Aqueous solution of 0.80 mol·L⁻¹ $MnCl_2$ was degassed before the mixing with Et_3N. Then 0.80 mol Et_3N was added to the degassed manganese chloride solution that caused the formation of white-gel precipitate. Crystallization of the fresh prepared precipitate resulted in amorphous sample not fitted for X-ray diffraction. So that the white-gel precipitate was kept for 72 h in a closed vessel to prevent it from the oxidation and after that it was crystallized. One main part of the powder obtained after crystallization of the white-gel precipitate has been identified with kempite structural analog, $Mn_2Cl(OH)_3$ according to X-ray diffraction analysis [12]. The other main part of the powder has been identified with the Mn^{II}-NEt₃ complex isolated from supernatant according to characteristic set of diffraction lines equally distanced via $2\Theta = 6.9° \pm 0.2°$ from each other in the diffractogramme [12].

2.3 Simultaneous AFM-SNOM and X-ray Diffraction

Simultaneous AFM-SNOM probing was applied in shear force mode with the equipment described in Ref. [16]. Light beam of argon laser emitting at 488 nm and spreading through an optical fiber was the light source. The feedback signal obtained from AFM setup was used for SNOM imaging. The variations of the light reflected back to the fiber of SNOM setup under the shear-force AFM control provide building up of SNOM image point by point. The tip was pulled with a Sutter Instrument, Model P-2000 Quartz Micropipette Puller [17]. Quartz glass tips with end radii of approximately 10 nm were applied to probe samples.

Detailed description of AFM-SNOM measurements can be found elsewhere [16].

Analysis of samples by XRD was carried out with the use of a DRON-2 diffractometer, which has the Cu anticathode with $K_{\alpha 1}$ line radiation ($\lambda = 1.54051$ Å). An estimate of the smallest in size particles, which were non-transparent for light in SNOM images, was performed for the particles by measurement of their diameter at contact with mica or PET surface. Thus, two modes of the particle diameter (d_s) measurement with the use of the cross-sections were applied to evaluate their size as displayed in Fig. 1. The resolution of the measurements has been defined using the cross-sections too, the smallest distance (d_{min}) between the neighboring dots in the profiles gave $d_{min} = 10.3 \pm 0.06$ Å with the reliability of 99%.

Thus, the resolution of the images obtained by simultaneous AFM-SNOM allowed to evaluate the size of the smallest particles settled down on the surface of mica or PET.

3. Results and Discussion

3.1 Simultaneous AFM-SNOM of Conjugated Mn^{III}-Hydroxide and Mn^{II}-NEt₃ Complex in Thin Layer

The interaction between Et₃N and MnCl₂ in alkaline aqueous solution results in the complex with formula $[Mn^{2+}(Et_3N)_3(H_3O)^+]Cl^-_3$ (Mn^{II}-NEt₃), which has 8 H₂O molecules in the coordination shell, conjugated with kempite structural analog, $Mn_2Cl(OH)_3$ [12]. Two different types of the particles self-assembled in the solution are usually observed by simultaneous AFM-SNOM, typical images of the first type particles are displayed in Fig. 2. Like for the particles formed by the complex of diethylamine and MnCl₂ [18] these particles of submicroscopic proportions observed by AFM are completely transparent for the light in the corresponding SNOM image. Detailed analysis of the particles of this type shows up very tiny non-transparent particles with the size of 65.1 ± 7.5 nm marked by an arrow in SNOM image of Fig. 2. The size of the particles has been evaluated with the reliability

of 99%. The smallest particles like those displayed in the cross-section in Fig. 2A or 2B are suitable for the size measurement, while the other particles contacting to each other usually lose their spherical shape.

The second type particles demonstrate the non-transparent for light core seen in the SNOM image in Fig. 3, the size of which was found within 300-400 nm at the half of the height [18] like that shown in the cross-section in Fig. 3A. In this case the smallest particles contacting with mica marked in the SNOM image and the cross-section in Fig. 3B are ranged in the 65.1 ± 7.5 nm interval with the reliability of 99%. The other particles contacting to each other lose their shape and form the body of the non-transparent compact core. Thus, the larger size particles and the submicroscopic core of 300-400 nm size have been self-assembled in the solution from the smallest grains that have diameter (d_s) ca. 65 nm at the contact with mica surface.

Crystal precursor before the crystallization in thin layer usually has plasticity parameter (σ) approximately 0.3 that has been found for microcrystal precursors of mono-protonated *meso*-tetraphenyl- porphine dimers self-organized into domain in thin layer due to the presence of confined water [11]. Such a low plasticity usually takes place because the precursor's inner structure, which has been self-organized in solution, is almost not deformed under contact with the support but
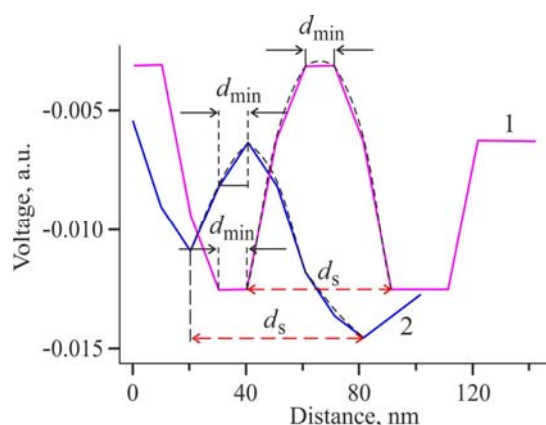
Fig. 1 Profiles of the smallest non-transparent particles obtained from SNOM images demonstrating two modes of the diameter (d_s) measurement; both can be approximated by a spherical segment with the same diameter at the contact with the support, see details in the text.
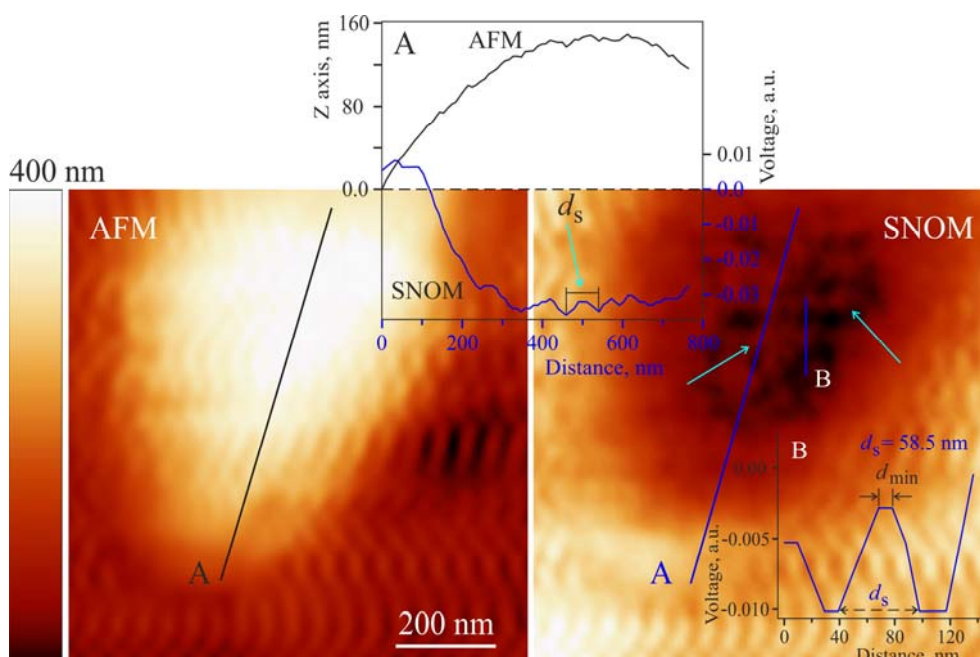
Fig. 2 Simultaneous AFM (0.9 μm × 0.9 μm), top view, z-scale: 400 nm and shear-force SNOM images (z-scale: voltage, 0.2 V) of the conjugate in thin layer with Et₃N ligand on mica. A letter denoting cross-section line drawn in the top view shows the origin of the cross-section in Fig. 2 and in the other figures except for Fig. 7.
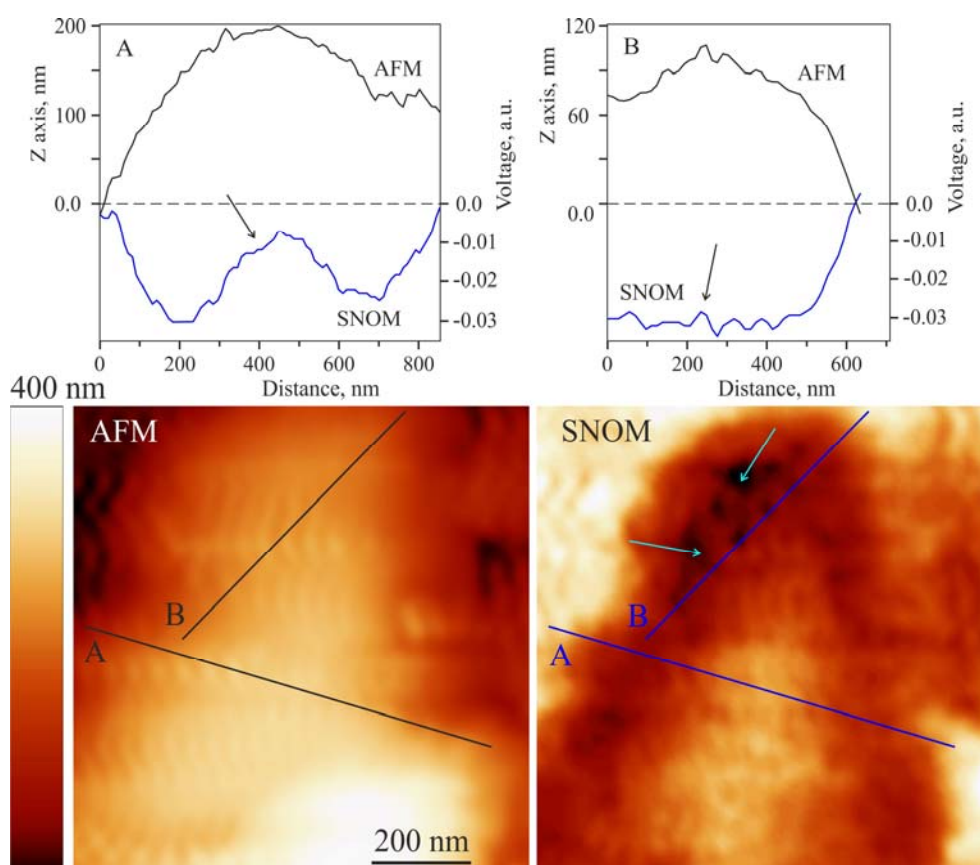

Fig. 3 Simultaneous AFM (0.9 μm × 0.9 μm), top view, z-scale: 400 nm and shear-force SNOM images (z-scale: voltage, 0.2 V) of the same thin layer prepared on mica as displayed in the caption of Fig. 2; the cross-section A intersects the core edge nearby B to show both in Fig. 3, see details in the text.

only an aqueous cover of the particle. The plasticity parameter of a particle is defined by Eq. (1), where d_s is the particle diameter at the surface contact and d_{es} is the diameter of the equivalent sphere [19].

$$\sigma = d_s /d_{es} - 1 \qquad (1)$$

So assuming $\sigma = 0.3$ for the crystal precursor with $d_s = 65.1$ nm we obtain $d_{es} = d_s/(\sigma + 1) = 50.1$ nm for the particles in aqueous solution with the self-organized inner structure because of hydrophobic Et$_3$N ligand. These particles with the average $d_{es} = 50.1$ nm are in consistent with crystallite size of 44.2 nm (see below XRD). It should be stressed that the crystallites of 44.2 nm size have been composed by Mn^{II}-NEt$_3$ complex and kempite structural analog that are compatible on molecular level producing the conjugate of Mn^{III}-hydroxide with Mn^{III}-NEt$_3$ complex [12]. Hence, the non-transparent submicroscopic core observed in SNOM image of Fig. 3 is rather self-assembled from these tiny particles closely contacting to each other in the core. In contrast, the first type particles, which are completely transparent for the light, mainly consist of kempite structural analog, Mn$_2$Cl(OH)$_3$ that is largely hydrated and admixture of the non-transparent smallest grains self-assembled from the conjugated Mn^{III}-hydroxide and Mn^{II}-NEt$_3$ complex.

It should be noted that the self-assembling of the smallest grains (ca. 65 nm) from the conjugate of [Mn^{2+}(Et$_3$N)$_3$(H$_3$O)$^+$]Cl$^-_3$ and Mn$_2$Cl(OH)$_3$ with the aqueous coordination shell, has mainly occurred in the solution due to the hydrogen bonding [12] and more likely hydrophobic interactions too. The latter play the determinative role in the larger particles selfassembling and the submicroscopic core, which is retained on hydrophilic mica surface as displayed in Fig. 3. However, no compact core was found when the thin layers were prepared on PET film, which is shown in Fig. 4. Therefore, in the latter case the core is destroyed on hydrophobic polyethylene terephthalate surface that contains the hydrophobic phenyl rings. So that the cross-sections demonstrate surface profiles like those found for Et$_2$NH-MnCl$_2$ complex, which did not

exhibit the core on hydrophilic mica surface because of the large hydration of this complex [18]. The smallest grains found under contact with PET film more likely consisting of the same conjugate because of its formation due to the hydrogen bonding, prefer to contact with the hydrophobic PET surface during the layer preparation. Thus, the separation of hydrophobic and hydrophilic surfaces has been destroyed and no ordered structure was found in the layers prepared on PET film.

Hence, the comparison of the images obtained on hydrophilic mica and hydrophobic PET surfaces allows to conclude that the non-transparent smallest grains self-assembling occurred due to the hydrogen bonding that dominates on the shorter distances. While the larger particles self-assembling including the compact submicroscopic core took place in the aqueous solution due to hydrophobic interactions. So that on hydrophilic mica surface, the core self-assembled from the smallest grains consisting of the Mn^{III}/Mn^{II}-based compounds prefers to stay in the intact form due to hydrophobic interactions between the grains.

3.2 Simultaneous AFM-SNOM of Mn^{III}/Mn^{II}-HNEt$_2$ Complex in Thin Layer

As reported earlier no compact core has been found for the complex formed in the result of the interaction between manganese chloride and diethylamine [18]. In this case the doublet at 1,046, 1,062 cm^{-1} of the complex, which is arisen from proton sharing in the C–N(H)...H$_3^+$O moiety, implies the formation of similar conjugate with Mn^{III}/Mn^{II} mixed states.

It follows from that the characteristic doublet responsible for proton sharing is shifted to the inherent frequency of ν(O–O) at 1,158 cm^{-1} observed in infrared spectra [18, 20]. It usually occurs at early steps of the interactions in the presence of dioxygen in solution until Mn^{III} is not oxidized yet. Thus, the smallest grains, the size of which falls in the 65 $\pm$ 7.5 nm interval observed in SNOM image of Fig. 5, are more likely formed due to the hydrogen bonding too.
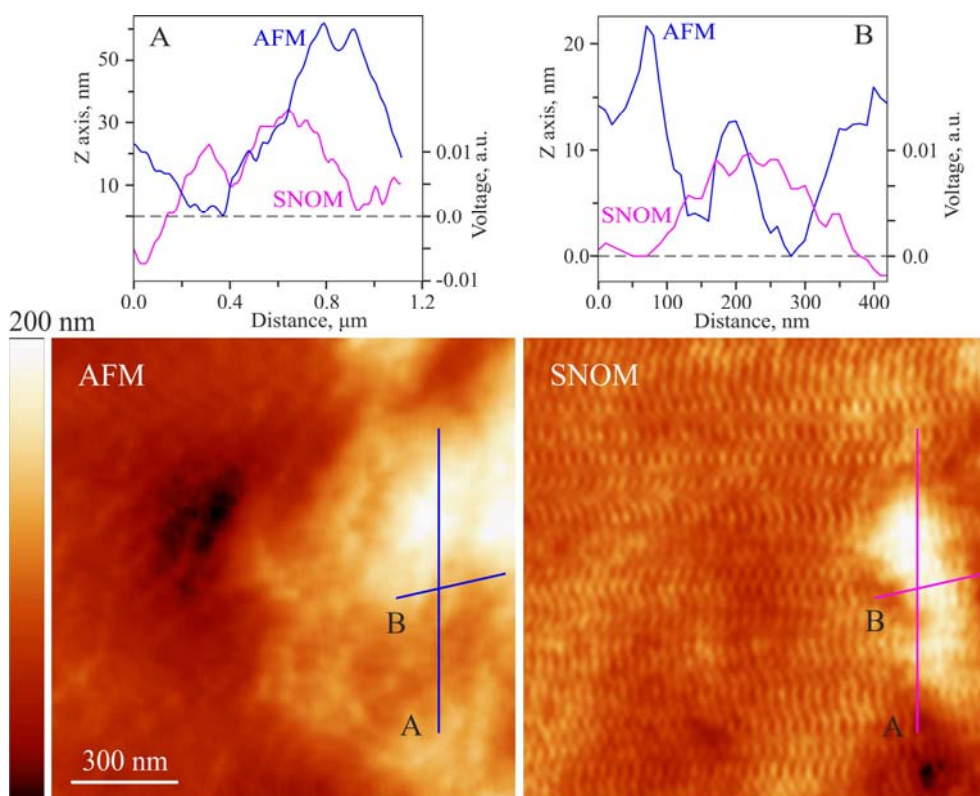
Fig. 4   Simultaneous AFM (1.7 μm × 1.7 μm), top view, z-scale: 200 nm and shear-force SNOM images (z-scale: voltage, 0.2 V) of the conjugate in thin layer prepared with Et₃N ligand on PET film with the same concentrations of 4.0×10^{-3} mol·L^{-1} MnCl₂ and 4.0×10^{-3} mol·L^{-1} Et₃N.

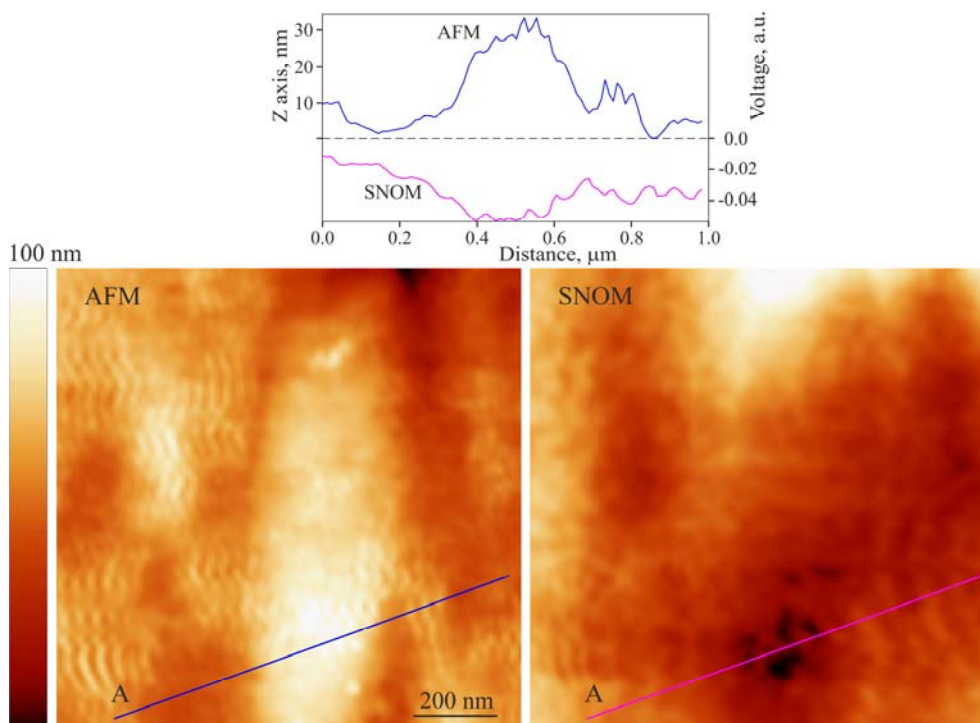**Fig. 5   Simultaneous AFM (1.1 μm × 1.1 μm), top view, z-scale: 100 nm and shear-force SNOM images (z-scale: voltage, 0.2 V) of a thin layer prepared by solvent evaporation from the solution 4.0×10^{-3} mol·L^{-1} MnCl₂ and 4.0×10^{-3} mol·L^{-1} Et₂NH on mica.**

This suggestion relatively to the hydrogen bonding under the self-assembly in solution is supported by similar smallest grains found in SNOM images of the layers of the same compounds prepared on PET film as displayed in Fig. 6. In this case, no compact submicroscopic core surrounded by the transparent for light aqueous cover is also found.

Thus, simultaneous AFM-SNOM of self-assembled compounds in thin layers prepared on hydrophilic mica surface and hydrophobic polyethylene terephthalate film can be successfully used to testify the self-assembly due to hydrophobic interactions. It is actually possible because the structuring with the hydrophobic phase separation occurs in solution that results in the formation of supramolecular structure covered by an aqueous coating. This way allows to observe the intact structure on hydrophilic mica surface like that found for the Mn^{II}-NEt₃ complex conjugated with kempite structural analog.

3.3 X-ray Diffraction of Mn^{III}-hydroxide Conjugated with Mn^{II}-NEt₃ Complex

As mentioned above the white-gel precipitate is the conjugate formed between kempite structural analog, $Mn_2Cl(OH)_3$ and complex including hydronium ion, $[Mn^{2+}(Et_3N)_3(H_3O)^+]Cl^-_3$. In the case of the particles with $d_s = 65$ nm being in the thin layer, the original their size in solution is 50 nm assuming that the plasticity parameter of the precursors is approximately 0.3 ($d_{es} = 65/(\sigma + 1) = 50$ nm). The crystallite size (D_{hkl}) after the crystallization of the molecular conjugate producing white-gel precipitate in solution can be estimated with the Scherrer's formula, (2) using the most intense diffraction lines displayed in Fig. 7.

$$D_{hkl} = 0.9 \ \lambda/(\beta cos\theta) \qquad (2),$$

where, λ is the X-ray wavelength (1.54051 Å), β is the full width at half maximum and θ is the Bragg's angle in radians both.

With $\theta = 0.1770$ rad (10.14°) and $\beta = 3.19 \times 10^{-3}$ the calculation gives $D_{hkl} = 44.2$ nm for the peak with d(Å) = 4.37 in Fig. 7, curve 2. With $\theta = 0.1784$ rad (10.22°)

and $\beta = 4.69 \times 10^{-3}$ the calculated $D_{hkl} = 30.0$ nm for the same peak in curve 1 of the water-soluble complex isolated from supernatant. In addition, for the kempite structural analog crystallized together with the water-soluble complex the calculated $D_{hkl} = 14.5$ nm is obtained with $\theta = 0.3269$ rad (18.73°) and $\beta = 1.01 \times 10^{-2}$. Thus, the sum of two latter crystallite sizes (30 + 14.5 = 44.5 nm) matches $D_{hkl} = 44.2$ nm of the conjugate that just means the both compounds are compatible on molecular level.

It should be noted that the Mn^{II}-NEt₃ complex isolated from supernatant manifests an intense band at 2,676 cm^{-1} in the infrared spectrum that is not observed for the Mn-based complex with Et₂NH [18]. The intense similar band at 2,665 cm^{-1} that is characteristic for so-called Eigen cation ($H_9O_4^+$) in gas phase has been assigned to asymmetric mode of H_3O^+ vibrations [21, 22]. The latter implies the hydronium ion (H_3O^+) rotation in the structure of the Mn^{II}-NEt₃ complex because of the asymmetric mode of the vibrations. Therefore, the distance between the second H_2O neighbors should be $d_{O-O,w} sin(\Theta/2)+d_{O-O,h} sin(\Theta/2)=$ 4.43 Å, where $d_{O-O,w}$ is the oxygen–oxygen distance between the neighboring H_2O molecules, $d_{O-O,w} =2.98$ Å [23], $\Theta = 109.5°$, and $d_{O-O,h}$ is the oxygen–oxygen distance in $H_5O_2^+$ ion, $d_{O-O,h} = 2.45$ Å, which provides equal probability for proton sharing in $H_5O_2^+$ ion and the proton delocalization in liquid water structure [24]. This distance d(Å) = 4.43 is observed as a shoulder in the X-ray diffraction pattern in Fig. 7, curve 1 of the complex. Thus, the water molecules composing the coordination shell retain tetrahedral coordination because of the hydrogen bonding.

Hence, the smallest particles of 65 nm size on average observed by SNOM for the conjugate of kempite structural analog with the Mn^{II}-NEt₃ complex including (H_3O)$^+$ ion are found in consistent with the crystallites size of 44.2 nm. The size of the corresponding precursors, which are deformed under contact with the surface, is estimated as $d_{es} = 50$ nm in solution. These size particles are produced in aqueous
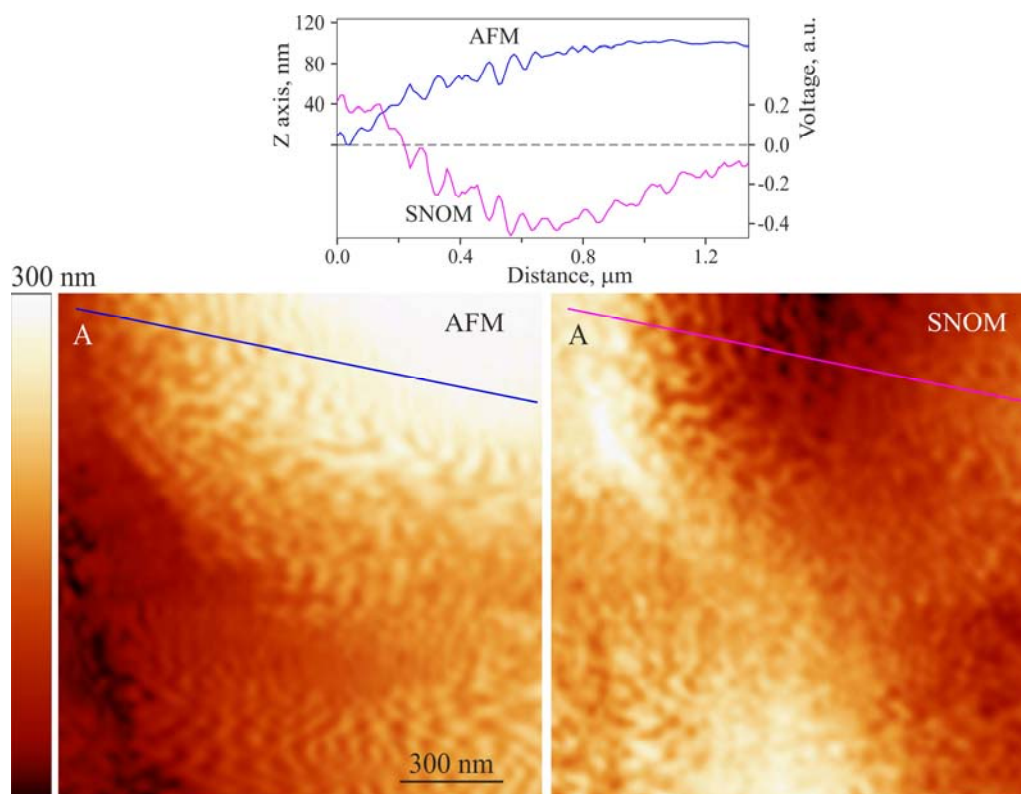
Fig. 6   Simultaneous AFM (1.4 μm × 1.4 μm), top view, z-scale: 300 nm and shear-force SNOM images (z-scale: voltage, 0.2 V) of similar thin layer as displayed in the caption of Fig. 5 but prepared on PET film.
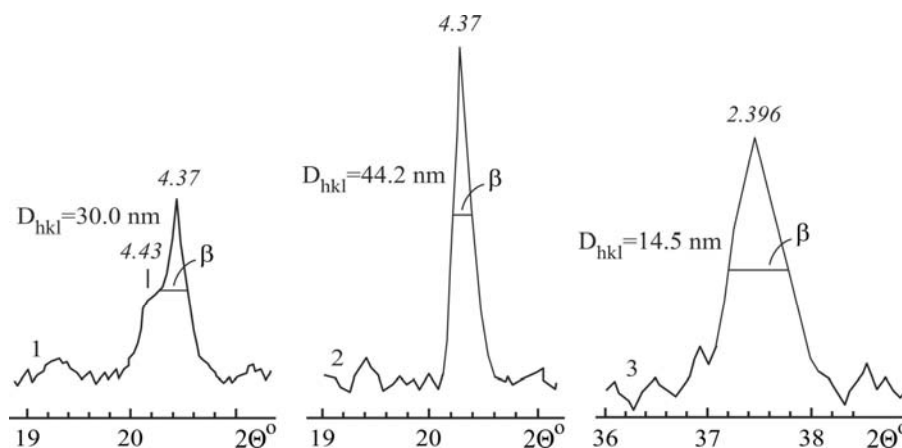

Fig. 7   The most intense diffraction lines found in X-ray diffraction patterns of: (1) yellow-green crystals of Mn^{II}-NEt₃ complex isolated from supernatant; and (2, 3) powder obtained after crystallization of white-gel precipitate, the peak with d_{hkl} = 2.396 Å has been identified with $Mn_2Cl(OH)_3$, kempite structural analog. The identification of kempite structural analog can be found in Ref. [12].

solution due to the hydrogen bonding between the ligands of Mn^{II}-NEt₃ complex and Mn^{III}-hydroxide.

4. Conclusions

Thus, behavior of $[Mn^{2+}(Et_3N)_3(H_3O)^+]Cl^-_3$ and $Mn_2Cl(OH)_3$ conjugated in solution with the formation

of the smallest particles of 65 ± 7.5 nm size observed by simultaneous AFM-SNOM is found independent on hydrophobic/hydrophilic surface of the support because of the self-assembling due to the hydrogen bonding. While the further self-assembling of the smallest particles producing submicroscopic compact

core that is non-transparent for light in the SNOM image is found dependent on hydrophilic mica surface and hydrophobic polyethylene terephthalate. In fact, on the latter surface, the smallest particles prefer to contact to hydrophobic surface that caused the submicroscopic compact core destroying. In contrast, similar compounds in the case of the complex with diethylamine, which is unable to form hydrophobic surface in aqueous solution, produce only the smallest particles of approximately the same size. Thus, simultaneous AFM-SNOM of the layers prepared on mica and PET surface can be used to testify the nature of the interactions under self-assembling of a compound in solution.

The crystallite size of 44.2 nm obtained with the use of X-ray diffraction for the former conjugated compounds is found in an agreement with the smallest grain size, 65 ± 7.5 nm measured at contact with the mica surface taking into account the precursor deformation. Therefore, the actual size of the smallest particles in the solution is ca. 50 nm on average that is in consistent with the crystallite size of 44.2 nm taking into consideration the liquid and solid their states.

Acknowledgment

References

[1] Kaupp, G. 2006. "Scanning Near-Field Optical Microscopy on Rough Surfaces: Applications in Chemistry, Biology, and Medicine." *Int. J. Photoenergy* 1-22.

[2] Sugimoto, Y., Pou, P., Abe, M., Jelinek, P., Pérez, R., Morita, S., and Custence, Ó. 2007. "Chemical Identification of Individual Surface Atoms by Atomic Force Microscopy." *Nature* 446: 64-7.

[3] Zheng, M., Zhang, H., Gong, X., Xu, R., Xiao, Y., Dong, H., Liu, X., and Liu, Y. 2013. "A Simple Additive-Free Approach for the Synthesis of Uniform Manganese Monoxide Nanorods with Large Specific Surface Area." *Nanoscale Res. Lett.* 8: 166-72.

[4] Sharrouf, M., Awad, R., Roumié, M., and Marhaba, S. 2015. "Structural, Optical and Room Temperature Magnetic Study of Mn_2O_3 Nanoparticles." *Materials Sci. Applicat.* 6: 850-9.

[5] Kaupp, G., Herrmann, A., and Haak, M. 1998. SNOM (Scanning Near-Field Optical Microscopy), a Genuine Photochemical Technique. *Internet Photochem. Photobiol.* 1998; http://www.photobiology.com/iupac98/gkaupp/snom.html (accessed Nov 25, 2016).

[6] Kaupp, G., Herrmann, A., Schmeyers, J., and Boy, J. 2001. "SNOM: A New Photophysical Tool." *J. Photochem. Photobiol. A: Chem.* 139: 93-6.

[7] Kajiyama, T., Tanaka, K., Ge, S.-R., and Takahara, A. 1996. "Morphology and Mechanical Properties of Polymer Surfaces via Scanning Force Microscopy." *Prog. Surface Sci.* 52: 1-52.

[8] Snitka, V., Rodaite, R., and Mizariene, V. 2005. "Self-assembly of $TPPS_4$ Porphyrin Molecules into Nanorods Investigated by TEM, AFM, STM and UV/VIS Spectroscopy." *NSTI- Nanotech.* 1: 789-92.

[9] Rojas, G., Chen, X., Bravo, C., Kim, J. H., Kim, J. S., Xiao, J., Dowben, P. A., Gao, Y., Zeng, X. C., Choe, W., and Enders, A. 2010. "Self-assembly and Properties of Nonmetalated Tetraphenyl-Porphyrin on Metal Substrates." *J. Phys. Chem. C.* 114: 9408-15.

[10] Kaupp, G. 2011. "The Enhancement Effect at Local Reflectance and Emission Back to Apertureless SNOM Tips in the Shear-Force Gap." *The Open Surface Sci. J.* 3: 20-30.

[11] Udal'tsov, A. V. 2016. "Germ Direct Observation by AFM under Crystallization of Self-organized Assemblies of Mono-Protonated *Meso*-Tetraphenylporphine Dimers." *J. Crys. Growth* 448: 6-16.

[12] Udaltsov, A. V., Lyutoev, V. P., and Belykh, D. V. 2016. "Hydrogen Bonding in Assemblies of Mn(II)/Mn(III)-NEt₃ Complex Self-organized with the Formation of Hydrophobic Core." *Key Engineer. Mater.* 708: 103-9.

[13] Glebov, E. M., Grivin, V. P., Plyusnin, V. F., Udal'tsov, A. V., Yiheng, Z., Herrmann, A., Kaupp, G., and Vos, J. G. 2005. "Manganese Complexes with Aliphatic Amines in Aqueous Solutions and in the Solid State." *Mendeleev's Communic.* 15: 17-9.

[14] Glebov, E. M., Grivin, V. P., Plyusnin, V. F., and Udal'tsov, A. V. 2006. "Manganese (II) Complexes with Diethylamine in Aqueous Solutions." *J. Structural Chem.* 47: 476-83.

[15] Cotton, F., and Wilkinson, J. 1969. *Modern Inorganic Chemistry*, Mir, Moscow, V. 3 (Russian).

[16] Kaupp, G. 2006. *Atomic Force Microscopy, Scanning Near-Field Optical Microscopy and Nanoscratching.* Berlin-Heidelberg-New York: Springer.

[17] Kaupp, G., Herrmann, A., and Wagenblast, G. 1999. "Scanning Near-Field Optical Microscopy (SNOM) with Uncoated Tips-Applications in Fluorescence Techniques and Raman Spectroscopy." In *Proc. of SPIE* 3706: 16-25, electronic version, http://kaupp.chemie.uni-oldenburg.de.

[18] Udal'tsov, A. V., Lyutoev, V. P., Belykh, D. V., and Vos, J. G. 2015. "Vibrational Characteristics of Triethylamine-Mn(II) Complex Self-assembled with the Formation of Hydrophobic Core in Comparison with Those of Diethylamine-Mn(II) Complex." *Vibr. Spectrosc.* 81: 53-61.

[19] Udal'tsov, A. V., Kaupp, G., and Taskaev, A. I. 2004. "Fine Surface Structure of Large-Scale Tetraphenylporphine Aggregates." *Colloid J.* 66: 489-94.

[20] Proniewicz, L. M., Bruha, A., Nakamoto, K., Kyuno, E., and Kincaid, J. R. 1989. "Resonance Raman Spectra of Dioxygen Adducts of Cobalt Porphyrin-Imidazole Complexes. Remarkable Spectroscopic Consequences of Hydrogen Bonding of the Coordinated Imidazole and the Lack of an Effect on the Cobalt-Oxygen Linkage." *J. Am. Chem. Soc.* 111: 7050-6.

[21] Headrick, J. M., Diken, E. G., Walters, R. S., Hammer, N. I., Christie, R. A., Cui, J., Myshakin, E. M., Duncan, M. A., Johnson, M. A., and Jordan, K. D. 2005. "Spectral Signatures of Hydrated Proton Vibrations in Water Clusters." *Science* 308: 1765-9.

[22] Kulig, W., and Agmon, N. 2014. "Both Zundel and Eigen Isomers Contribute to the IR Spectrum of the Gas-Phase $H_9O_4^+$ Cluster." *J. Phys. Chem. B* 118: 278-86.

[23] Stillinger, F. H. 1980. "Water Revisited." *Science* 209: 451-7.

[24] Udal'tsov, A. V., Bolshakova, A. V., and Vos, J. G. 2015. "The Role of Zundel-like Ions in the Supramolecular Self-organization of Porphyrin Assemblies." *J. Mol. Struct.* 1080: 14-23.